

## Gain-Feedback Approach to Optical Instabilities in Sodium Vapor

G. Khitrova, J. F. Valley, and H. M. Gibbs

*Optical Sciences Center, University of Arizona, Tucson, Arizona 85721*

(Received 11 December 1987)

The gain-feedback approach to lasing and optical instabilities has been applied to sodium vapor driven by a nearly resonant intense field. The observed lasing frequencies agree with the two-beam-coupling gain curve calculated for a Doppler-broadened two-level medium. Rayleigh-gain lasing is seen for no external cavity with use of counterpropagating beams, and Raman-gain lasing is seen in a ring cavity.

PACS numbers: 42.65.Ma, 32.80.Wr, 42.50.Tj, 42.65.Ky

Silberberg and Bar-Joseph<sup>1-4</sup> have analyzed the onset of an optical instability as the simultaneous occurrence of sufficient gain and feedback to permit lasing at a new frequency.<sup>5</sup> The instability observed on the transmitted light is then merely the beat between the pump field and the newly generated "lasing." We have used this gain-feedback approach in sodium vapor<sup>4</sup> using the Rayleigh gain to generate sideband lasing displaced from the driving laser field by 8 to 14 MHz. Raman-gain lasing is also seen, but it is displaced by the on-resonance Rabi frequency, typically 4 GHz or less here, rather than by the effective Rabi frequency which is larger because of the detuning. The new observations are Rayleigh-gain lasing with no external mirrors with use of counterpropagating pump beams,<sup>1,4</sup> Rayleigh-gain lasing without a foreign gas,<sup>6</sup> and Raman-gain lasing in a ring cavity.

The pump-probe or two-beam-coupling gain curve for a stationary Na atom has already been derived<sup>7,8</sup> and verified.<sup>9</sup> Here we adopt the nomenclature of Haroche and Hartman<sup>7</sup> and refer to the dispersion-shaped resonance at the laser frequency  $\nu_L$  as "Rayleigh" (called  $1/T_1$  in Ref. 4) and the gain peak at  $\nu_L - \nu_{RE}$  as "Raman" (sometimes called Rabi<sup>4</sup> or three-photon<sup>10</sup> gain). Here the effective Rabi frequency is  $\nu_{RE} = (|\delta\nu_L|^2 + \nu_R^2)^{1/2}$ , where  $\nu_R$  is the on-resonance Rabi frequency,  $\delta\nu_L = \nu_L - \nu_0$ , and  $\nu_0$  is the two-level-atom frequency. For moving atoms, one must integrate this curve over the velocity distribution; this has been expressed as easily calculable sums of plasma dispersion functions.<sup>11-13</sup> Figure 1 compares the detuned stationary-atom curve in Fig. 1(a) with the Doppler-broadened curve in Fig. 1(b) showing the ac Stark shift of the absorption peak and the shift and broadening of the Raman gain. The peak of the Raman gain occurs at a frequency  $\nu$  given by  $\nu \cong \nu_L \pm \nu_{RE}$  for a stationary atom, where  $\pm$  is given by  $\delta\nu_L/|\delta\nu_L|$ . For moving atoms and when the Doppler broadening is roughly equal to  $\delta\nu_L$ , as in Fig. 1(b), the Raman gain is much broader and its peak shifts to almost  $\nu_L - \nu_R$ . In contrast, the Rayleigh gain is Doppler free and hardly affected. Lasing will be described on the basis of these two gain mechanisms with use of two different feedback configurations.

The experimental apparatus consists of a cw ring dye

laser and sodium cell. The  $\cong 900$ -mW single-mode output power of the dye laser is diffracted from an acousto-optic Bragg cell so that any feedback is shifted by 80 MHz and has no effect on the dye-laser frequency. The beam is then spatially filtered, collimated, and focused by a 30- or 45-cm focal-length lens into the sodium with a maximum of 700 mW reaching the Na. For most of the measurements the Na cell was a flow cell with a 9-mm length of the Na; the argon pressure was usually  $\leq 0.3$  Torr. A 10-cm evacuated quartz cell was used to show Rayleigh-gain lasing at zero pressure. Beat frequencies up to 300 MHz could be observed with a photodiode and a Hewlett-Packard model 8568B spectrum analyzer. A Fabry-Perot interferometer (flat mirrors with  $R \cong 0.98$ ) was used to study lasing at frequencies differing from  $\nu_L$  by more than 100 MHz. The detuning  $\delta\nu_L$  is measured with Lamb-dip spectroscopy, and zero is defined as the center of the strongest (here the nearest) hyperfine transition.

For the counterpropagating-beams case, 300-mW beams were focused by two 30-cm focal-length antireflection-coated lenses; see Fig. 2 inset. Two new observations with counterpropagating-beams distributed feedback (DFB) were made: an optical instability by means of Rayleigh-gain lasing with no external cavity, and Rayleigh-gain lasing with zero foreign-gas pressure. The observation of mirrorless self-oscillation (i.e., lasing) is shown in Fig. 2. The zeroth-order DFB modes of our short samples are broad and essentially flat over the Rayleigh-gain region which peaks at about 10 MHz from  $\nu_L$ ; consequently, lasing occurs at the peak of the gain curve. The lengths  $L$  here, 0.9 cm for the flow cell and 10 cm for the quartz cell, are both short compared with the long lengths proposed in Ref. 4, where the next-higher-order DFB mode at  $c/2L$  is made to coincide with the Rayleigh-gain curve. Mirrorless lasing was reported previously in the pulsed regime in semiconductor crystals; because the processes were frequency degenerate, a small angle was required between the counterpropagating pumps in order to distinguish the lasing.<sup>14</sup> Here, the  $\cong 10$ -MHz frequency shift facilitates detection by the heterodyne technique even for exact counterpropagation. Note that the generation mechanism for

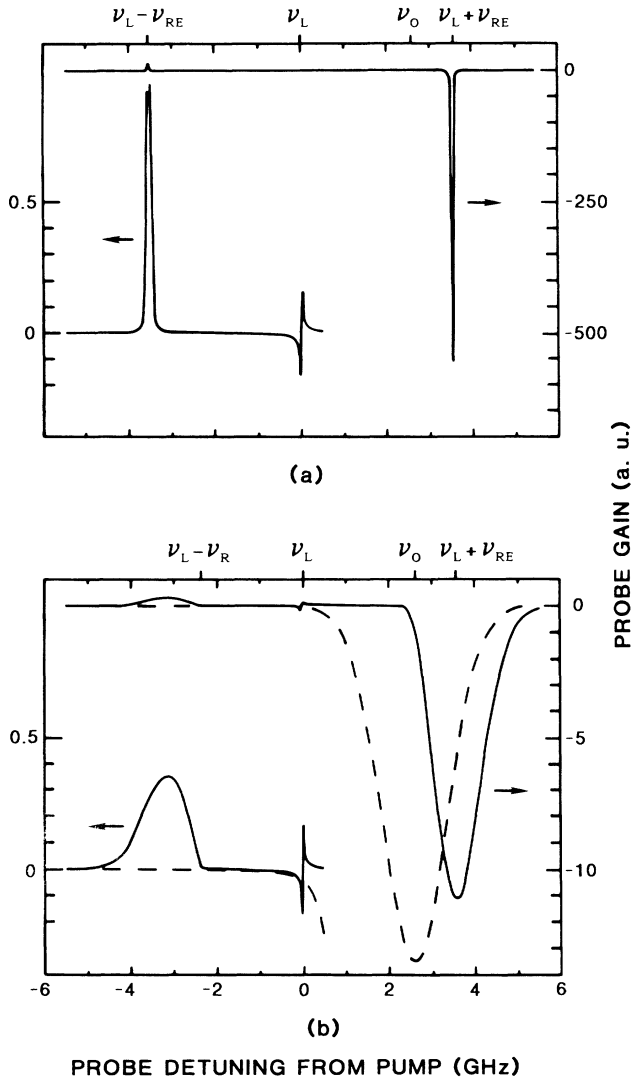


FIG. 1. Calculations (Ref. 11) of (a) the stationary-atom and (b) the Doppler-broadened probe-gain profiles for an intense pump at  $\nu_L$  detuned by  $\nu_L - \nu_0 = -2.6$  GHz (defocusing side) from the low-field line center  $\nu_0$ . The Rabi frequency is  $\nu_R = 2.4$  GHz and the argon pressure 0.3 Torr. The abbreviation "a.u." stands for "arbitrary units." (a) The well-known ac-Stark-shifted absorption at  $\nu_L + \nu_{RE}$ . The 500 $\times$  enlargement at the left shows Raman gain (peak value 14) at  $\nu_L - \nu_{RE}$  and Rayleigh gain peaked at about  $(2\pi T_1)^{-1}$  to the right of  $\nu_L$ . (b) For a Doppler width of 2 GHz, one sees that the high-intensity absorption (solid curve) is shifted from the low-intensity absorption (dashed curve). [The 10 $\times$  enlargement at the left has the same scale as the enlargement in (a), showing that the Rayleigh gain near  $\nu_L$  is hardly affected.] But the Raman gain has a lower peak and greater width enabling several modes to lase as shown in Fig. 3.

Rayleigh-gain lasing at  $\nu_L + f$  is a two-beam coupling, but nearly degenerate four-wave mixing results in  $\nu_L - f$  in the counterpropagating-beams case.

The second DFB observation, namely Rayleigh-gain

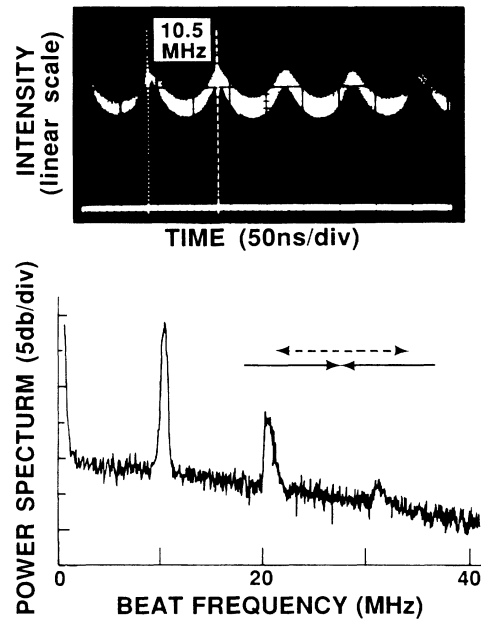


FIG. 2. Time dependence and power spectrum of one of the counterpropagating pump beams after passing through the sodium vapor for  $\delta\nu_L \cong -2.6$  GHz (defocusing side). The  $f = 10.5$  MHz beat frequency arises mostly from lasing at the peak at  $\nu_L + f$  of the Rayleigh gain and from emission at  $\nu_L - f$ ; the 21-MHz peak is the beat between  $\nu_L - f$  and  $\nu_L + f$ . Inset: Geometry of the counterpropagating pumps (solid arrows) and Rayleigh lasing (dashed arrows).

lasing without foreign gas, was performed in the evacuated 10-cm Na cell. It emphasizes that a closed system (i.e., no collisions and no decay to an external reservoir) with large detuning can exhibit Rayleigh gain. In terms of a perturbation-expansion susceptibility, Rayleigh gain occurs in fifth order with no foreign gas and in third order with foreign-gas pressure.<sup>6,11,12</sup> Thus the zero-pressure Rayleigh-gain lasing requires more pump power than with pressure. This may explain why Grandclément, Grynberg, and Pinard<sup>15</sup> observed Rayleigh lasing only with pressure using Na in a ring cavity.<sup>16</sup>

For the ring-cavity experiments, three highly reflecting flat mirrors and two 30-cm focal-length antireflection-coated lenses were used to form a ring cavity for the lasing with  $L = 98$  cm; see Fig. 3 inset. The input was focused by a 45-cm lens, resulting in a 112- $\mu$ m waist  $w [I = I_0 \exp(-2r^2/w^2)]$  in the Na. Since the pump beam passes through the Na in only one direction, there are no counterpropagating beams. Lasing occurs in only one direction in the cavity, namely in the forward direction with respect to the pump, because of the Doppler effect. In the case of a probe beam propagating in a direction opposite to the pump beam, the averaging over the velocity distribution reduces the gain strongly. For  $\delta\nu_L = -4.1$  GHz, the Raman-gain lasing at  $\nu$  begins at  $\nu_L - \nu = 4$  GHz, just slightly larger than the  $\nu_R \cong 3.7$  GHz calculated from the 680-mW input power, the

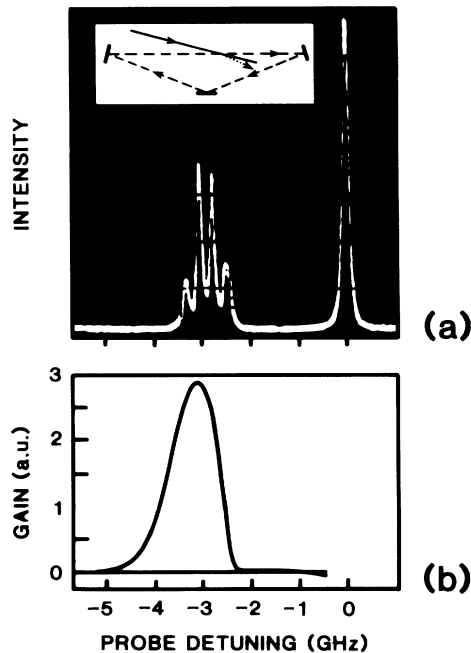


FIG. 3. Raman-gain lasing in Na in a ring cavity (see inset) for  $\delta\nu_L \cong -2.6$  GHz (defocusing side). (a) Fabry-Perot spectrum showing laser light (injected external to the ring cavity) at  $\nu - \nu_L = 0$  and lasing of four Raman-gain ring-cavity modes for  $\nu - \nu_L \cong -3$  GHz. (b) Raman-gain calculated curve from Fig. 1(b). [Note that the arbitrary units ("a.u.") here are 8 times those of Fig. 1(b)].

112- $\mu\text{m}$  waist, and the dipole moment<sup>9</sup> of Na. This 4-GHz shift of the Raman lasing from  $\nu_L$  is much less than the 5.7 GHz it would be if the atoms were stationary. Because of the broadened gain curve, several longitudinal modes of the ring cavity may be above the Raman lasing threshold, as shown in Fig. 3(a) for  $\delta\nu_L = -2.6$  GHz. The mode spacings range from 240 to 270 MHz, different from  $c/L = 306$  MHz because of dispersion. Comparison with the calculated plane-wave gain curve is made in Fig. 3(b), where  $\nu_R = 2.4$  GHz gives a better fit because of absorption and defocusing. The lasing has a waist of only 67  $\mu\text{m}$  in the sodium and makes an angle of about  $0.9^\circ$  relative to the pump beam, so that it uses the gain in the uniform portion of the pump beam. This justifies the use of the plane-wave gain curve. Rayleigh-gain lasing in the ring cavity was also seen, as already reported by Grandclément, Grynberg, and Pinard.<sup>15</sup> It is interesting to note that two-beam coupling is common in photorefractive crystals. In fact, Rayleigh-gain lasing has been seen with use of a bismuth silicon oxide (BSO) photorefractive crystal in a ring cavity; the peak is shifted by only about 30 Hz.<sup>17</sup> The non-local photorefractive effect (diffusion limit) gives one  $\pi/2$  phase shift, and the grating reflection for the Bragg condition gives another  $\pi/2$  phase shift; together they add to the  $\pi$  phase shift needed for optimum transfer. Here

there is no transfer for  $\nu = \nu_L$  because the detuned two-level-medium polarization is local and in phase with the stationary light grating. But for a probe detuned by about 10 MHz, the light grating moves, causing the Na polarization to lag behind just enough to make the scattered beam in phase with the probe, as needed for the most efficient transfer.

Note that the ring-cavity lasing observed here is unidirectional, so that counterpropagation<sup>18</sup> instabilities do not occur. Both the ring-cavity and counterpropagating-beams lasings observed here have the same linear polarization as the pump(s), and so the polarization instability of Gaeta *et al.* and Kaplan and Law<sup>19</sup> did not occur. In fact, they use a nonlinear-medium description that does not apply to sodium vapor, as pointed out by Ducloy and Bloch.<sup>20</sup>

A signal field oscillating at  $\nu_3 = \nu_L + f$  may interact with the strong field at  $\nu_L$  to generate by forward four-wave mixing a field at  $\nu_4 = 2\nu_L - \nu_3 = \nu_L - f$ , or vice versa.<sup>10,21,22</sup> If the signal wave travels at an angle  $\theta$  relative to the pump wave, then the generated wave will travel in the direction dictated by phase matching (roughly  $-\theta$  for  $\theta = 0.9^\circ$ ).<sup>21</sup> Consequently, the ring-cavity emission does not include the complements of the Rayleigh and Raman lasings; however, those emissions are seen outside the cavity at the phase-matched angle. But in the counterpropagating-beams case, emissions are seen at both  $\nu_L \pm f$  because the beams are essentially collinear (see Fig. 2) and both backward and forward four-wave mixing can contribute.

In summary, the gain-feedback approach is a stimulating alternative to direct probe-absorption measurements. Even more importantly, it is a powerful tool for the study of the onset of optical instabilities. One can even manipulate the frequencies of the instabilities by controlling the interplay between the gain and feedback frequency profiles.

The authors are grateful for fruitful discussions with P. Berman, Y. Silberberg, G. Giusfredi, S. L. McCall, K. Tai, E. Ressayre, M. LeBerre, and A. Tallet, and to the National Science Foundation (Grants No. PHY 8602306 and No. INT 8612339), the U.S. Air Force Office of Scientific Research, and the U.S. Army Research Office for support.

<sup>1</sup>Y. Silberberg and I. Bar-Joseph, Phys. Rev. Lett. **48**, 1541 (1982).

<sup>2</sup>I. Bar-Joseph and Y. Silberberg, Opt. Commun. **48**, 53 (1983).

<sup>3</sup>Y. Silberberg and I. Bar-Joseph, J. Opt. Sci. Am. B **1**, 662 (1984).

<sup>4</sup>I. Bar-Joseph and Y. Silberberg, Phys. Rev. A **36**, 1731 (1987).

<sup>5</sup>Of course, several authors have recognized that self-oscillations can arise from the amplification of sidebands: S. L.

McCall, Phys. Rev. A **9**, 1515 (1974); A. C. Tam, Phys. Rev. A **19**, 1971 (1979); S. T. Hendow and M. Sargent, III, Opt. Commun. **40**, 485 (1982); L. W. Hillman, R. W. Boyd, and C. R. Stroud, Jr., Opt. Lett. **7**, 426 (1982); W. J. Firth, E. M. Wright, and E. J. D. Cummins, in *Optical Bistability 2*, edited by C. M. Bowden, H. M. Gibbs, and S. L. McCall, (Plenum, New York, 1983), p. 111. The Raman gain here is the origin of the self-pulsing predicted by R. Bonifacio and L. A. Lugiato, Lett. Nuovo Cimento **21**, 510 (1978), and seen by B. Segard and B. Macke, Phys. Rev. Lett. **60**, 412 (1988).

<sup>6</sup>P. R. Berman, G. Khitrova, and J. F. Lam, in *Spectral Line Shapes*, edited by F. Rostas (de Gruyter, Berlin, 1985), Vol. 3, p. 337; G. Grynberg, E. Le Bihan, and M. Pinard, J. Phys. (Paris) **47**, 1321 (1986).

<sup>7</sup>S. Haroche and F. Hartman, Phys. Rev. A **6**, 1280 (1972).

<sup>8</sup>B. R. Mollow, Phys. Rev. A **5**, 2217 (1972).

<sup>9</sup>F. Y. Wu, S. Ezekiel, M. Ducloy, and B. R. Mollow, Phys. Rev. Lett. **38**, 1077 (1977). For a full discussion, see M. D. Levenson, *Introduction to Nonlinear Laser Spectroscopy* (Academic, New York, 1982), Sect. 3.1.

<sup>10</sup>R. W. Boyd, M. G. Raymer, P. Narum, and D. J. Harter, Phys. Rev. A **24**, 411 (1981).

<sup>11</sup>G. Khitrova, Ph.D. dissertation, New York University, 1986, unpublished. Eqs. (4.1)–(4.6) on pp. 54–57 were used to generate Figs. 1 and 3(b);  $v_R$  here is  $2X/2\pi T_1$  there. Only a single two-level transition is assumed, but inclusion of both hyperfine components affects the gains very little for negative detuning.

<sup>12</sup>G. Khitrova, P. Berman, and M. Sargent, III, J. Opt. Soc.

Am. B **5**, 160 (1988).

<sup>13</sup>Pump-probe measurements of the Doppler-broadened gain profile are reported in M. T. Gruneisen, K. R. MacDonald, and R. W. Boyd, J. Opt. Soc. Am. B **5**, 123 (1988).

<sup>14</sup>S. G. Odulov, S. S. Slydsarenko, and M. S. Soskin, Kvantovaya Elektron. (Moscow) **11**, 869 (1984) [Sov. J. Quantum Electron. **14**, 589 (1984)].

<sup>15</sup>D. Grandclément, G. Grynberg, and M. Pinard, Phys. Rev. Lett. **59**, 40, 44 (1987).

<sup>16</sup>A pressure-induced extra resonance was observed in four-wave mixing by Y. Prior, A. R. Bogdan, M. Dagenais, and N. Bloembergen, Phys. Rev. Lett. **46**, 111 (1981). In contrast, the zero-pressure Rayleigh-gain lasing here uses two-wave mixing.

<sup>17</sup>H. Rajbenbach and J. P. Huignard, Opt. Lett. **10**, 137 (1985).

<sup>18</sup>A. E. Kaplan and P. Meystre, Opt. Commun. **40**, 229 (1982).

<sup>19</sup>A. E. Gaeta, R. W. Boyd, J. R. Ackerhalt, and P. W. Milonni, Phys. Rev. Lett. **58**, 2431 (1987); A. E. Kaplan and C. T. Law, IEEE J. Quantum Electron. **21**, 1529 (1985).

<sup>20</sup>M. Ducloy and D. Bloch, Phys. Rev. A **30**, 3107 (1984). For further discussion and experimental confirmation, see P. R. Berman, D. G. Steel, G. Khitrova, and J. Liu, Phys. Rev. A, to be published.

<sup>21</sup>B. R. Mollow, Phys. Rev. A **7**, 1319 (1973).

<sup>22</sup>Gain at  $v_L \pm v_{RE}$  was reported in the stationary-atom limit by D. J. Harter, P. Narum, M. G. Raymer, and R. W. Boyd, Phys. Rev. Lett. **46**, 1192 (1981).

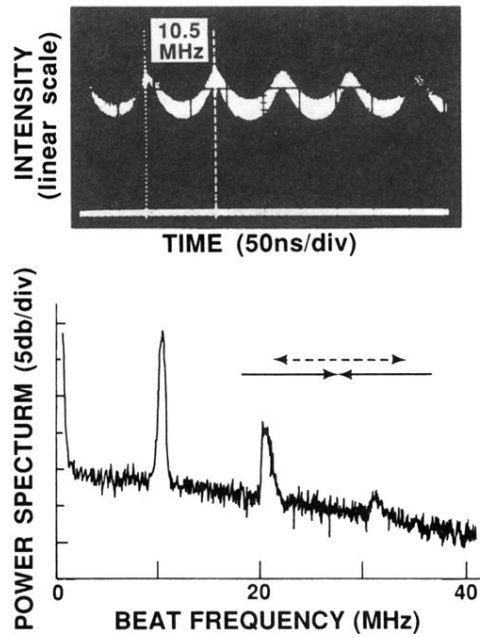


FIG. 2. Time dependence and power spectrum of one of the counterpropagating pump beams after passing through the sodium vapor for  $\delta\nu_L \cong -2.6$  GHz (defocusing side). The  $f=10.5$  MHz beat frequency arises mostly from lasing at the peak at  $\nu_L + f$  of the Rayleigh gain and from emission at  $\nu_L - f$ ; the 21-MHz peak is the beat between  $\nu_L - f$  and  $\nu_L + f$ . Inset: Geometry of the counterpropagating pumps (solid arrows) and Rayleigh lasing (dashed arrows).

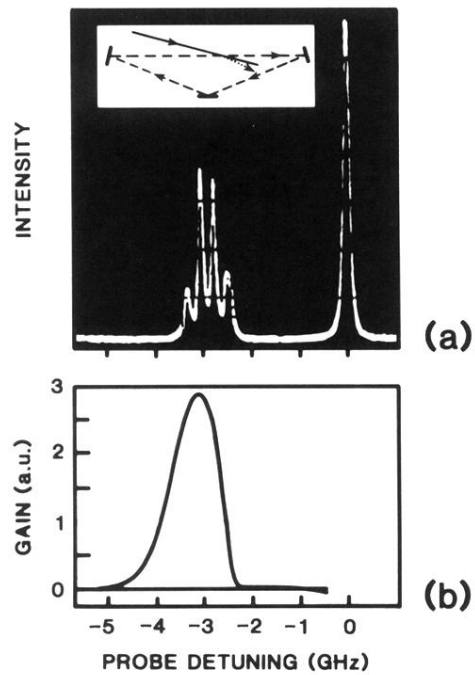


FIG. 3. Raman-gain lasing in Na in a ring cavity (see inset) for  $\delta\nu_L \cong -2.6$  GHz (defocusing side). (a) Fabry-Perot spectrum showing laser light (injected external to the ring cavity) at  $\nu - \nu_L = 0$  and lasing of four Raman-gain ring-cavity modes for  $\nu - \nu_L \cong -3$  GHz. (b) Raman-gain calculated curve from Fig. 1(b). [Note that the arbitrary units ("a.u.") here are 8 times those of Fig. 1(b)].